

# On Touching Triangle Graphs

Emden R. Gansner<sup>1</sup>, Yifan Hu<sup>1</sup>, and Stephen G. Kobourov<sup>2</sup>

<sup>1</sup> AT&T Labs - Research, Florham Park, NJ

<sup>2</sup> University of Arizona, Tucson, AZ

**Abstract.** In this paper, we consider the problem of representing graphs by triangles whose sides touch. We present linear time algorithms for creating touching triangle representations for outerplanar graphs, square grid graphs, and hexagonal grid graphs. The class of graphs with touching triangle representations is not closed under minors, making characterization difficult. We do show that pairs of vertices can only have a small common neighborhood, and we present a complete characterization of the subclass of biconnected graphs that can be represented as triangulations of some polygon.

## 1 Introduction

Planar graphs are a widely studied class that includes naturally occurring subclasses such as trees and outerplanar graphs. Typically planar graphs are drawn using the node-link model, where vertices are represented by points and edges are represented by line segments. Alternative representations, such as contact circles [2] and contact triangles [7] have also been explored. In these representations, a vertex is a circle or triangle, and an edge is represented by pairwise contact at a common point.

In this paper, we explore the case where vertices are polygons, with an edge whenever the sides of two polygons touch. Specifically, given a planar graph  $G = (V, E)$ , we would like to find a set of polygons  $R$  such that:

1. there is bijection between  $V$  and  $R$ ;
2. two polygons touch non-trivially if and only if the corresponding vertices are adjacent in  $G$ ;
3. and each polygon is convex.

Note that, unlike the case of contact circle and contact triangle representations, two polygons that share a common point are not considered adjacent. It is easy to see that all planar graphs have representations meeting conditions 1 and 2 above, as pointed out by de Fraysseix *et al.* [6]. Starting with a straight-line planar drawing of  $G$ , a polygon for each vertex can be defined by taking the midpoints of all adjacent edges and the centers of all neighboring faces. The *complexity*, i.e., number of its sides, of the resulting polygons can be as high as  $|V| - 1$ , as it is proportional to the degree of the corresponding vertex. Moreover, the polygons would not necessarily be convex.

A theorem of Thomassen [19] implies that all planar graphs can be represented using convex hexagons and this also follows from results by Kant [14] and de Fraysseix *et al.* [6]. Gansner *et al.* [9] have shown that six sides are not only sufficient but also necessary, and gave a linear time and area construction. This leads us to consider which planar graphs can be represented by polygons with fewer than six sides.

This paper presents some initial results for the case of touching triangles. We assume we are dealing with connected planar graphs  $G = (V, E)$ . We let  $TTG$  denote the class of graphs that have a touching triangle representation. Concerning how to attack the problem, we can start with some simple observations. First, unlike such classes as planar graphs,  $TTG$  graphs are not closed under homeomorphisms or minors (cf. Appendix). On the other hand, as Corollary 1 shows, we can sometimes find a subclass of  $TTG$  graphs which can be extended by homeomorphism. In addition, there is the special subclass of *filled*  $TTG$  graphs, i.e., those for which the polygon formed by the union of triangles is simply-connected. At times, the filled version can be more tractable than the general version, and may lead to a solution of the general problem [3].

In Section 2, we show that all outerplanar graphs can be represented as filled  $TTG$ . Similarly, we show in Section 3 that all subgraphs of a square or hexagonal grid are in  $TTG$ . All of these representations can be computed in linear time. Section 4 characterizes the special case of graphs arising from filled triangulations of polygons. Finally, in Section 5, we show that, for graphs in  $TTG$ , pairs of vertices can have very limited common neighborhoods. This allows us to identify concrete examples of graphs not in  $TTG$ .

## 1.1 Related Work

Results on representing planar graphs as “contact systems” can be dated back to Koebe’s 1936 theorem [15] which states that any planar graph can be represented as a contact graph of disks in the plane. When the regions are further restricted to rectangles, not all planar graph can be represented. Rahman *et al.* [17] describe a linear time algorithm for constructing rectangular contact graphs, if one exists. Buchsbaum *et al.* [3] provide a characterization of the class of graphs that admit rectangular contact graph representation. The version of the problem where it is further required that there are no holes in the rectangular contact graph representation is known as the rectangular dual problem. He [11] describes a linear time algorithm for constructing a rectangular dual of a planar graph, if one exists. Kant’s linear time algorithm for drawing degree-3 planar graphs on a hexagonal grid [14] can be used to obtain hexagonal drawings for planar graphs. Gansner *et al.* [9] show that at least six sides are necessary and that the lower bound is matched by an upper bound of six sides with a linear time algorithm for representing any planar graph by touching convex hexagons.

In VLSI floor-planning it is often required to partition a rectangle into rectilinear regions so that non-trivial region adjacencies correspond to a given planar graph. It is natural to try to minimize the complexities of the resulting regions and the best known results are due to He [12] and Liao *et al.* [16] who show that regions need not have more than 8 sides. Both of these algorithms run in  $O(n)$  time and produce layouts on an integer grid of size  $O(n) \times O(n)$ , where  $n$  is the number of vertices.

Rectilinear cartograms can be defined as rectilinear contact graphs for vertex weighted planar graphs, where the area of a rectilinear region must be proportional to the weight of its corresponding node. Even with this extra condition, de Berg *et al.* [4] show that rectilinear cartograms with constant region complexity can be constructed in  $O(n \log n)$  time. Specifically, a rectilinear cartogram with region complexity 40 can always be found.

## 2 Outerplanar Graphs

In this section, we show that any outerplanar graph can be represented by a set of touching triangles, that is, outerplanar graphs belong to the class  $TTG$ . Here we assume that we are given an outerplanar graph  $G = (V, E)$  and the goal is to represent  $G$  as a set of touching triangles. We describe a linear time algorithm based on inserting the vertices of  $G$  in an easy-to-compute “peeling” order.

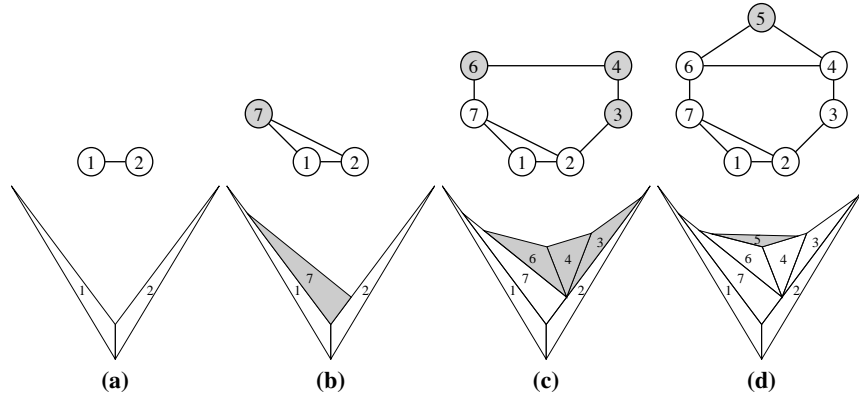


**Fig. 1.** Incremental construction of the  $TTG$  representation for outerplanar graphs. The shaded vertices on the top row and shaded regions on the bottom row are the ones processed at the current step.

### 2.1 Algorithm Overview

1. Compute an outerplanar embedding of  $G$ .
2. Compute a reverse “peeling” order of chains of vertices of  $G$ .
3. Insert region(s) corresponding to the current set of vertices in the peeling order, while maintaining a concave upper envelope.

We now look at each step in more detail. First we compute an outerplanar embedding of the graph, that is, an embedding in which all the vertices are on the outer face. For a given planar graph  $G = (V, E)$ , this can be easily done in linear time as follows. Let  $w$  be a new vertex and let  $G' = (V', E')$ , where  $V' = V \cup \{w\}$  and  $E' = E \cup \{(v, w) \mid v \in V\}$ . Note that  $G'$  is planar: if it contained a subgraph homeomorphic to  $K_5$  or  $K_{3,3}$ , then  $G$  would contain a subgraph homeomorphic to  $K_4$  or  $K_{3,2}$ , which would imply that  $G$  was not outerplanar to begin with as these are forbidden graphs for outerplanar graphs (Theorem 11.10, [10]). We can then compute a planar embedding for  $G'$  with  $w$  on the outer face. Removing  $w$  and all its edges yields the desired outerplanar embedding, with all vertices on the outer face.

The second step of the algorithm is to compute a reverse “peeling” order of the vertices of  $G$ . Such an order is defined by peeling off one face at a time and keeping

track of the set of removed vertices. If  $G$  is a single edge, the result is trivial, so we may assume that  $|V| > 2$ . In addition, we may assume that  $G$  is biconnected. If not, we can traverse the outer face  $v_1, v_2, \dots, v_n$ . If we encounter a node  $v_i = v_j, 1 < j < i$ , we add a new node  $w_i$  and edges  $(v_{i-1}, w_i)$  and  $(w_i, v_{i+1})$ . The graph remains outerplanar, and we continue the traversal from  $v_{i+1}$ . This yields a biconnected graph  $G'$ . If we can construct a TTG for  $G'$ , we need only remove the triangles corresponding to the added vertices to get a TTG for  $G$ .

The dual of an outerplanar graph restricted to the interior faces is a tree. We pick a face with at least one edge  $(v_1, v_2)$  on the outer face and make that the root of the tree. We then remove the faces in depth-first order. At each step, a face consists of vertices  $v, u_1, u_2, \dots, u_j, w$ , where  $j \geq 1$  and only the edge  $(w, v)$  is part of another face. We then remove the path  $u_1, u_2, \dots, u_j$  and continue the process until we come to the root face. We then remove the path connecting  $v_1$  and  $v_2$ .

The third step of the algorithm is to create the touching triangles representation of  $G$ , by processing the graph using the peeling order from the second step. We begin by placing the vertices  $v_1$  and  $v_2$  as shown in Fig. 1(a). We then recreate each face in the reverse order in which it was removed by adding triangles corresponding to the path removed from the face. We assume that, at each step, we have the following two invariants:

1. each pair of adjacent triangles corresponding to the path from  $v_1$  to  $v_2$  form a concave angle
2. each triangle has part of its upper side forming part of the boundary.

This is clearly true for the first step.

Suppose the path being added consists of a single vertex  $w$  connecting to adjacent vertices  $v_i$  and  $v_k$ . Let  $p$  be the point where triangles  $v_i$  and  $v_k$  meet concavely, and let  $q$  and  $r$  be any two points of the exposed upper sides of the two triangles  $v_i$  and  $v_k$ . We can then add  $w$  as the triangle  $p, q, r$ , giving us the next face and maintaining the invariants. This is illustrated in Figures 1(b) and (d).

If the path to be added consists of multiple vertices  $u_1, u_2, \dots, u_j$ , with  $u_1$  and  $u_j$  connecting to adjacent vertices  $v_i$  and  $v_k$ , respectively, we again let the points  $p, q, r$  be as defined in the previous paragraph. We then pick points  $s_1, s_2, \dots, s_{j-1}$  so that path  $q, s_1, s_2, \dots, s_{j-1}, r$  is a concave path of line segments. We can then add this face using the triangles

$$(q, p, s_1), (s_1, p, s_2), \dots, (s_{j-2}, p, s_{j-1}), (s_{j-1}, p, r)$$

while maintaining the invariants. Figure 1(c) shows a sample of this.

Figure 1 provides an example of the algorithm. We start with the outerplanar embedding shown in the top line of Figure 1(d), and progressively remove chains until we are left with a single edge. This is used to create the configuration shown at the bottom of Fig. 1(a). The chains are added as fans of triangles until we finish with the *TTG* shown at the bottom right.

The first step of this algorithm can be done in linear time as it is a slight modification of a standard planar embedding algorithm such as that by Hopcroft and Tarjan [13]. The second step can also be done in linear time as computing the “peeling ordering”

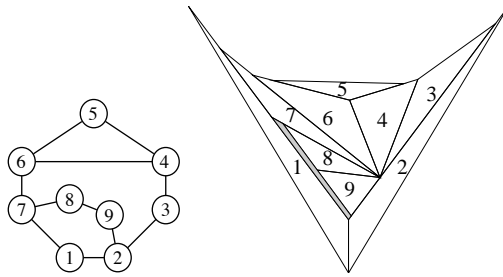


Fig. 2. Replacing a chord in an outerplanar graph with a path

requires constant time per face, given the embedding of the graph from the previous step. In the third step, we record the three edges of each triangle corresponding to each processed vertex. Inserting a new chain of vertices involves finding, say, the midpoint of the exposed edges, and forming the “fan” of new triangles, all tasks which require constant time per vertex and add up to linear overall time. Thus, we have the following theorem:

**Theorem 1.** *A touching triangles representation can be computed in linear time for any outerplanar graph.*

Given that the above construction relies on fitting chains of triangles into smaller and smaller areas with each face, the area bounds are likely to be poor.

**Corollary 1.** *Any graph homeomorphic to an outerplanar graph has a touching triangles representation.*

**Proof:** (Sketch) Without loss of generality, we may assume that  $G$  is biconnected with an embedding such that all vertices are on the outer face except for paths of nodes connecting two nodes on the outer cycle. We then replace these interior chains by chords, yielding an outerplanar graph, and use the algorithm described above. By the construction, any chord is represented by two triangles, one of whose sides is totally within a side of the other. The shorter side can then be rotated, breaking the chord but leaving all other adjacencies intact. It is then simple to insert a fan of triangles corresponding to replacing the chord by a path of nodes. Figure 2 shows how the edge between nodes 2 and 7 in Figure 1(d) can be replaced by a chain of two nodes.  $\square$

### 3 Grid Graphs

In this section, we show that any subgraph of a square or hexagonal grid graph can be represented by a set of touching triangles. We describe a linear time algorithm based on inserting the vertices of the graph in an outward fashion starting from an interior square/hexagon. We illustrate the algorithm with examples in Figure 3.

#### 3.1 Algorithm Overview

We first consider *TTG* representations for grid graphs.

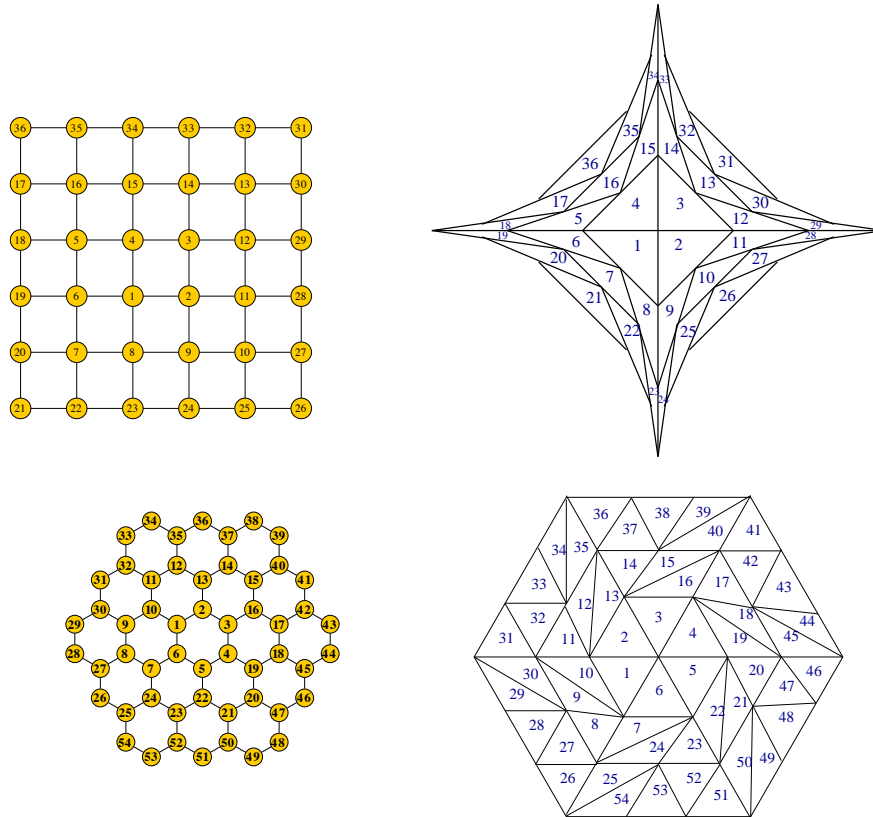


**Fig. 3.** Grid graphs (left) as touching triangles (right). The Hamiltonian path that visits all the vertices in the spiral order is given by the labels of the vertices.

1. Compute a planar embedding of  $G$ .
2. Compute a “spiral” order of the vertices of  $G$ .
3. Insert region(s), corresponding to a vertex or a path of vertices in the spiral order, while maintaining a concave upper envelope in each quadrant (in the case of square grid), or by carving out triangles out of trapezoids that correspond to the current spiral segment (in the case of hexagonal grid).

The first step of the algorithm is to compute a planar embedding of the graph, which can be done in linear time [13]. Next we compute a “spiral” order of the vertices. Such an order is defined by a Hamiltonian path which starts with the innermost face and visits all the vertices as shown in Fig. 3. Note that this is well defined for symmetric grid graphs but can be modified to handle asymmetric grid graphs and subgraphs of grid graphs.

In the case of square grids, the plane is partitioned into four quadrants and in each quadrant the spiral order introduces vertices in paths of increasing lengths  $(1, 3, 5, \dots)$ . In general these paths can be introduced recursively, provided that the upper envelope of the quadrant remains concave. The insertion of regions is similar to the process described for outerplanar graphs above.

In the case of hexagonal grids the plane is partitioned into six sectors and in each sector the spiral order introduces vertices in paths of increasing lengths (1, 3, 5, ...). In general, these paths can be introduced directly by adding an adjacent trapezoidal region and carving it into triangles.

The above algorithms show how to construct a *TTG* representation for any square or hexagonal grid graph. To get a *TTG* representation for any subgraph, one need only remove the triangles corresponding to vertices unused in the subgraph, and adjust the remaining triangles to remove any contacts corresponding to unused edges. Thus, we have the following theorem:

**Theorem 2.** *A touching triangles representation can be computed in linear time for any subgraph of a square or hexagonal grid graph.*

## 4 Triangulations

If we require each face in a triangle representation to have exactly three vertices, i.e., the vertex of one triangle cannot touch the side of another, we get the special case of *TTGs* we call *triangulation graphs*. These representations clearly correspond to creating a triangular mesh [1, 5], allowing Steiner points within the interior of a polygon. For example, the representation in the bottom right of Fig. 3 is a triangulation graph and the representation in the top right of Fig. 3 is not.

It is easy to see that triangulation graphs form a strict subset of *TTGs*. For example,  $K_4$  is a *TTG* but not a triangulation graph. It is also immediate that a triangulation graph has maximum degree 3, because by the definition of triangulation graphs, the vertex of one triangle cannot touch the side of another.

**Lemma 1.** *If  $G$  is a triangulation graph with no nodes of degree 1,  $G$  has at least 3 nodes of degree 2.*

**Proof:** The only triangles that can contribute to the polygon's boundary or outer face must have degree 2 in the graph, each contributing exactly 1 edge to the boundary. Since the polygon has at least 3 edges, the result follows.  $\square$

Here we focus on the *filled triangulation graphs*, those whose *TTG* representation is filled. It is possible to fully characterize the biconnected subset of these graphs.

**Theorem 3.** *A biconnected graph  $G$  is a filled triangulation graph if and only if it has:*

1. *only nodes of degree 2 or 3*
2. *an embedding in the plane such that:*
  - (a) *every internal node has degree 3;*
  - (b) *there are at least 3 nodes of degree 2 on the boundary;*
  - (c) *if there are any degree 3 nodes on the boundary, all of the degree 2 nodes cannot be consecutive; and*
  - (d) *if the degree 2 nodes on both ends of a chain of degree 3 boundary nodes are removed, the graph remains connected.*

**Proof:** We first prove necessity. Let  $G$  be a filled triangulation graph. Since it is biconnected, it cannot have any vertices of degree 1. Its triangulation representation yields an embedding with all internal nodes of degree 3. Lemma 1 shows we have at least 3 nodes of degree 2 on the boundary.

Suppose there are degree 3 nodes on the boundary and the degree 2 nodes are consecutive. The chain of degree 2 nodes cannot connect at a single vertex, because this would be a cut vertex. Thus, if we remove all triangles corresponding to degree 2 nodes, we would have a triangulation representation of a graph with exactly 2 vertices of degree two, which is not allowed by Lemma 1.

To finish the proof of necessity, we note that for two degree 2 triangles to disconnect the triangulation, they would have to share an interior vertex. On the other hand, if all intervening triangles on the boundary have degree 3, they can contribute nothing to the polygon boundary, so the two degree 2 must share another vertex. But then, they share a side, so there can't be any intervening degree 3 triangles.

Next, we prove sufficiency. We assume  $G$  is biconnected, all of its vertices have degree 2 or 3, and it has the specified embedding. We construct a graph  $G'$  which is a special kind of dual of  $G$ .  $G'$  contains the dual of the interior faces and edges of  $G$ . In addition,  $G'$  has a vertex for each maximal sequence of degree 3 nodes on the boundary, and a vertex for each boundary edge connecting two degree 2 nodes. These are placed in the external face of  $G$ , near the corresponding nodes or edges. These vertices are connected in a cycle of  $G'$  following the ordering induced by the boundary nodes and edges of  $G$ . Finally, for each boundary edge  $e$  of  $G$ , we add an edge from the node of  $G'$  corresponding to the interior face of  $G$  containing  $e$  to one of the vertices on the external cycle of  $G'$ . If  $e$  is adjacent to a vertex of degree 3, we connect the edge to the node of  $G'$  corresponding to the degree 3 vertex. Otherwise, we connect to the node of  $G'$  corresponding to  $e$ .

It is immediate from the construction that  $G'$  is a planar embedding of nodes and edges; all interior faces are triangles; and there is a 1-1 correspondence between faces of  $G'$  and vertices of  $G$  and between edges in  $G$  and  $G'$ . We need to show that  $G'$  is a simple graph.

As  $G$  is biconnected,  $G'$  can have no loops. Property 2(d) of the embedding implies that each interior face is connected to at most one of the nodes associated with the exterior face. The only way that multiedges could then occur would be if  $G'$  has a boundary consisting of two nodes and two edges. We know  $G$  has at least  $n_2 \geq 3$  nodes of degree 2 on the boundary. If there are only degree 2 nodes on the boundary,  $G'$  has a boundary of  $n_2$  nodes. Assume  $G$  has some degree 3 nodes on the boundary. If these nodes split into 3 or more paths, the construction creates at least 3 nodes on the boundary of  $G'$ . If not, they must split into 2 paths, since the degree 2 nodes must be separated. One group of degree 2 nodes must contain at least 2 nodes. The construction then creates one node for each group of degree 3 nodes, and at least one node for the path of more than 2 degree nodes, again given  $G'$  at least 3 boundary nodes.

As  $G'$  is simple, by using one of the algorithms (e.g, [8]) for making the edges of planar graph into line segments while retaining the embedding, we derive a triangulation representation of  $G$ , completing the proof.  $\square$

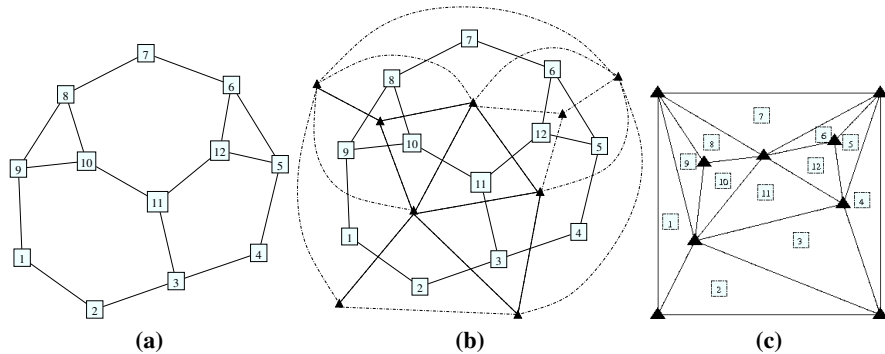


**Fig. 4.** Constructing a triangulation graph. (a) Original graph; (b) Creating the “dual” graph; (c) Straightening the edges.

Perhaps not surprisingly, the conditions of the theorem have a similar feel to those for rectangular drawings [17]. It is also not hard to see that the result can probably be derived from the duality between planar, cubic, 3-connected graphs and triangulations of the plane [18], but our proof seems more straightforward. Lastly, we note that Theorem 3 gives another proof that the hexagonal grid graphs of Section 3 have a touching triangle representation.

Figure 4 illustrates the algorithm. Figure 4(a) shows a graph satisfying the conditions of the theorem. In Figure 4(b), we have added a node for each internal face, and node on the outside for each sequence of degree 3 nodes or for each edge both of whose nodes have degree 2. This gives us a planar graph with each face having three sides and associated with a node of the original graph. Straightening the sides of the faces makes each face a triangle.

## 5 Necessary conditions

Thus far, we have shown that various categories of graphs are in  $TTG$ . Now, we wish to pursue some necessary conditions which will eliminate many graphs from  $TTG$ . Specifically, we show that pairs of vertices in any graph that can be represented by touching triangles must have a small common neighborhood: if a pair of vertices is connected by an edge, they cannot have more than 3 common neighbors, and if they are not directly connected, they cannot have more than 4 common neighbors. We start with some definitions.

Given triangles  $T_0$  and  $T_1$ , pick two sides  $s_0$  and  $s_1$ , one from each triangle, and orient the side counter-clockwise around the interior of the triangle. Extend the sides into directed lines  $L_0$  and  $L_1$ . If the lines intersect at a unique point, the intersection is *feasible* if a non-trivial portion of  $s_0$  lies to the right of  $L_1$  and a non-trivial portion of  $s_1$  lies to the right of  $L_0$ . Of the four angles formed at a feasible intersection, there is a unique one corresponding to a right turn. We call this a *feasible angle*. Two sides are *collinear* if the directed lines  $L_0$  and  $L_1$  are identical.

**Lemma 2.** *If a triangle  $T$  touches both  $T_0$  and  $T_1$ , using two distinct sides, one of its angles must be a feasible angle of  $T_0$  and  $T_1$ .*

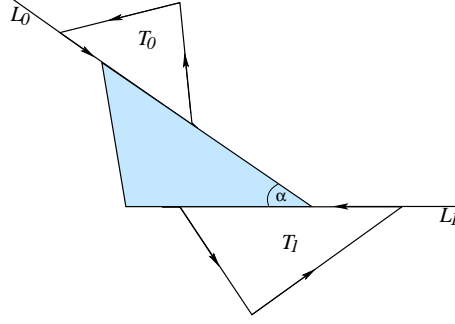


**Fig. 5.** A triangle  $T$  touching two other triangles  $T_0$  and  $T_1$ . The angle  $\alpha$  is a feasible angle of  $T_0$  and  $T_1$ .

**Proof:** If  $\alpha$  is the angle of  $T$  determined by the two touching sides of  $T_0$  and  $T_1$ , it is immediate that  $\alpha$  is a feasible angle. See Figure 5.  $\square$

This lemma already greatly reduces the possible  $TTG$  graphs. If two triangles have no collinear sides, there can be at most nine triangles touching both of them, since any such triangle eliminates at least one of the feasible angles. If two sides are collinear, one triangle can touch those two sides. Any other triangles must correspond to feasible angles, and since the remaining sides of both triangles are all to the left of the two collinear sides, there can be at most 4 feasible angles. We next work at tightening these bounds.

For a node  $u$  in  $G$ , we let  $N_u$  be the nodes in  $G$  joined to  $u$  by an edge. If  $u$  and  $v$  are two nodes in a graph  $G$ , define  $N_{uv}$  as the mutual neighbors of  $u$  and  $v$ , that is,  $N_{uv} = N_u \cap N_v$ . Finally, define  $E_{uv}$  be the subset of edges of  $G$  induced by  $N_{uv}$ .

**Theorem 4.** Let  $G$  be a  $TTG$ , and let  $u$  and  $v$  be two nodes in  $G$  joined by an edge. Then  $|N_{uv}| \leq 3$  and  $|E_{uv}| \leq 1$ .

**Proof:** Let  $T_u$  and  $T_v$  be the two triangles corresponding to nodes  $u$  and  $v$ . Since the two nodes share an edge,  $T_u$  and  $T_v$  must touch. There are basically two possibilities: one side is totally contained in the other or not.

In the first case, we have the situation represented in Figure 6. We immediately note that there can be no feasible angle associated with  $\vec{12}$  and  $\vec{ab}$ . In addition,  $\vec{ab}$  is to the left of both  $\vec{23}$  and  $\vec{31}$ . On the other hand, there are feasible angles formed by  $\vec{12}$  with  $\vec{bc}$  and  $\vec{ca}$ . So, we only have to consider pairings of  $\vec{23}$  and  $\vec{31}$  with  $\vec{bc}$  and  $\vec{ca}$ .

If point  $c$  is placed in region II, both  $\vec{bc}$  and  $\vec{ca}$  are to the left of  $\vec{23}$  and  $\vec{31}$ , so there are no more feasible angles, giving a total of two.

If  $c$  is in region III, we get a new feasible angle formed by  $\vec{31}$  and  $\vec{bc}$ . In this case, though, we are left with  $\vec{bc}$  and  $\vec{ca}$  to the left of  $\vec{23}$ , and  $\vec{31}$  to the left of  $\vec{ca}$ . Thus, we have at most three feasible points. We also note that any triangle associated with the feasible angle formed by  $\vec{12}$  and  $\vec{ca}$  cannot share an edge with any triangle of the other two feasible angles, so there can be at most one edge among the neighbors of  $u$  and  $v$ . The argument is similar if  $c$  is in region I.

If points 1 and  $b$  are identical, the same arguments hold except, in addition, we no longer have a feasible angle formed by  $\vec{12}$  and  $\vec{bc}$  because  $\vec{12}$  is to the left of  $\vec{bc}$ . Thus,

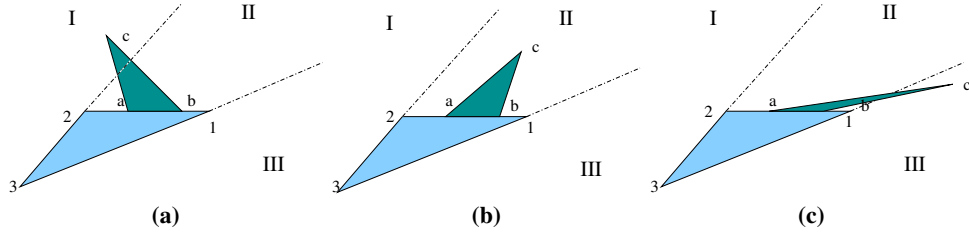


**Fig. 6.** Touching triangles with one side contained in the other. (a) Node  $c$  in region I; (b) Node  $c$  in region II; (c) Node  $c$  in region III.

we have at most two mutual neighbors and no edge between them. If points 2 and  $a$  are the same, the same arguments hold. Putting these two cases together, we find that if 1 and  $b$  are identical and 2 and  $a$  are identical, there can be at most one feasible angle.

The remaining case occurs when neither shared side is contained in the other. This is the situation represented by Figure 7.

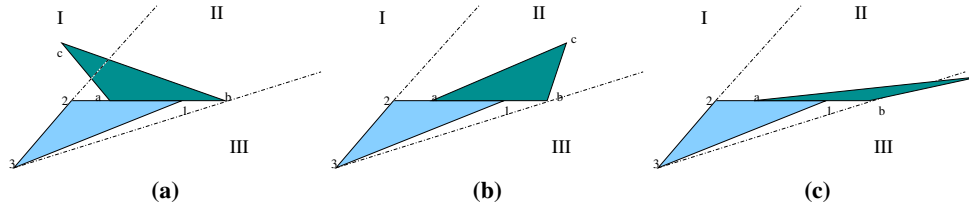


**Fig. 7.** Touching triangles with touching sides overlapping. (a) Node  $c$  in region I; (b) Node  $c$  in region II; (c) Node  $c$  in region III.

As previously, there can be no feasible angle associated with  $\vec{12}$  and  $\vec{ab}$ , but now we have feasible angles formed by  $\vec{12}$  and  $\vec{ca}$ , and by  $\vec{31}$  and  $\vec{ab}$ . In addition,  $\vec{12}$  is to the left of  $\vec{bc}$  and  $\vec{ab}$  is to the left of  $\vec{23}$ . Again, we are reduced to considering the four pairings of  $\vec{23}$  and  $\vec{31}$  with  $\vec{bc}$  and  $\vec{ca}$ . If  $\vec{ca}$  is to the right of  $\vec{31}$ , then  $\vec{31}$  is to the left of  $\vec{ca}$ , and vice versa, so that pairing is not possible. Finally, we note that if  $c$  is in regions I or II, then  $\vec{23}$  and  $\vec{31}$  are to the left of  $\vec{bc}$ , while if  $c$  is in regions II or III,  $\vec{bc}$  and  $\vec{ca}$  are to the left of  $\vec{23}$ . So, if  $c$  is in region II, there are at most two feasible angles. Otherwise, there can be three but, as above, at most two of the associated triangles can touch.  $\square$

We next consider what happens to the set of common neighbors if we relax the condition that there is an edge between two nodes.

**Theorem 5.** *Let  $G$  be a TTG, and let  $u$  and  $v$  be any two nodes in  $G$ . Then  $|N_{uv}| \leq 4$  and  $|E_{uv}| \leq 2$ .*

**Proof:** The proof is similar to that of Theorem 4; see the Appendix for details.  $\square$

## 6 Conclusion and Future Work

We considered the class of graphs that can be represented as contact graphs of triangles, and showed that this includes outerplanar graphs, as well as subgraphs of square

and hexagonal grids. We derived some necessary conditions for such TTG graphs, and described a complete characterization of biconnected triangulation graphs.

A complete characterization of graphs in *TTG*, as well as contact graphs of 4-gons and 5-gons, remains open. This is true even for the typically simpler case where “holes” are not allowed. Theorem 3 does solve the no-hole problem for a restricted version of *TTG* graphs. Can this be extended to allow for holes? Finally, the work on hexagonal contact graphs [9] gives a small ( $|V| \times |V|$ ) area bound. Are small areas possible in the triangular or, at least, the outerplanar case?

## References

1. M. Bern. Triangulations. In J. E. Goodman and J. O’Rourke, editors, *Handbook of Discrete and Computational Geometry*, CRC Press, 1997. 1997.
2. G. R. Brightwell and E. R. Scheinerman. Representations of planar graphs. *SIAM Journal on Discrete Mathematics*, 6(2):214–229, May 1993.
3. A. L. Buchsbaum, E. R. Gansner, C. M. Procopiuc, and S. Venkatasubramanian. Rectangular layouts and contact graphs. *ACM Transactions on Algorithms*, 4(1), 2008.
4. M. de Berg, E. Mumford, and B. Speckmann. On rectilinear duals for vertex-weighted plane graphs. *Discrete Mathematics*, 309(7):1794–1812, 2009.
5. M. de Berg, M. van Kreveld, M. H. Overmars, and O. Schwarzkopf. *Computational Geometry: Algorithms and Applications*. Springer-Verlag, 2nd edition, 2000.
6. H. de Fraysseix, P. O. de Mendez, and P. Rosenstiehl. On triangle contact graphs. *Combinatorics, Probability and Computing*, 3:233–246, 1994.
7. H. de Fraysseix, P. O. de Mendez, and P. Rosenstiehl. Representation of planar hypergraphs by contacts of triangles. In *15th Symposium on Graph Drawing*, pages 125–136, 2007.
8. H. de Fraysseix, J. Pach, and R. Pollack. Small sets supporting Fary embeddings of planar graphs. In *20th Symposium on Theory of Computing (STOC)*, pages 426–433, 1988.
9. E. Gansner, Y. Hu, M. Kaufmann, and S. Kobourov. Optimal polygonal representation of planar graphs. In *9th LATIN Symposium*, pages 417–32, 2010.
10. F. Harary. *Graph Theory*. Addison-Wesley, Reading, MA, 1972.
11. X. He. On finding the rectangular duals of planar triangulation graphs. *SIAM Journal of Computing*, 22(6):1218–1226, 1993.
12. X. He. On floor-plan of plane graphs. *SIAM Journal of Computing*, 28(6):2150–2167, 1999.
13. J. Hopcroft and R. E. Tarjan. Efficient planarity testing. *Journal of the ACM*, 21(4):549–568, 1974.
14. G. Kant. Hexagonal grid drawings. In *18th Workshop on Graph-Theoretic Concepts in Computer Science*, pages 263–276, 1992.
15. P. Koebe. Kontaktprobleme der konformen Abbildung. *Berichte über die Verhandlungen der Sächsischen Akademie der Wissenschaften zu Leipzig. Math.-Phys. Klasse*, 88:141–164, 1936.
16. C.-C. Liao, H.-I. Lu, and H.-C. Yen. Compact floor-planning via orderly spanning trees. *Journal of Algorithms*, 48:441–451, 2003.
17. M. Rahman, T. Nishizeki, and S. Ghosh. Rectangular drawings of planar graphs. *Journal of Algorithms*, 50(1):62–78, 2004.
18. E. Steinitz and H. Rademacher. *Vorlesungen über die Theorie der Polyeder*. Springer-Verlag, Berlin, 1934.
19. C. Thomassen. Plane representations of graphs. In J. A. Bondy and U. S. R. Murty, editors, *Progress in Graph Theory*, pages 43–69. Academic Press, Canada, 1984.

## Appendix

### Non-TTG Planar Graphs

Here we briefly illustrate that the property “representable as *TTG*” is not closed under homeomorphisms or minors. Specifically, the graphs in the top row of Figure 8 cannot be represented as *TTGs*, due to Theorems 4 and 5. On the other hand, subdividing one edge from each of them makes them representable as *TTGs*.

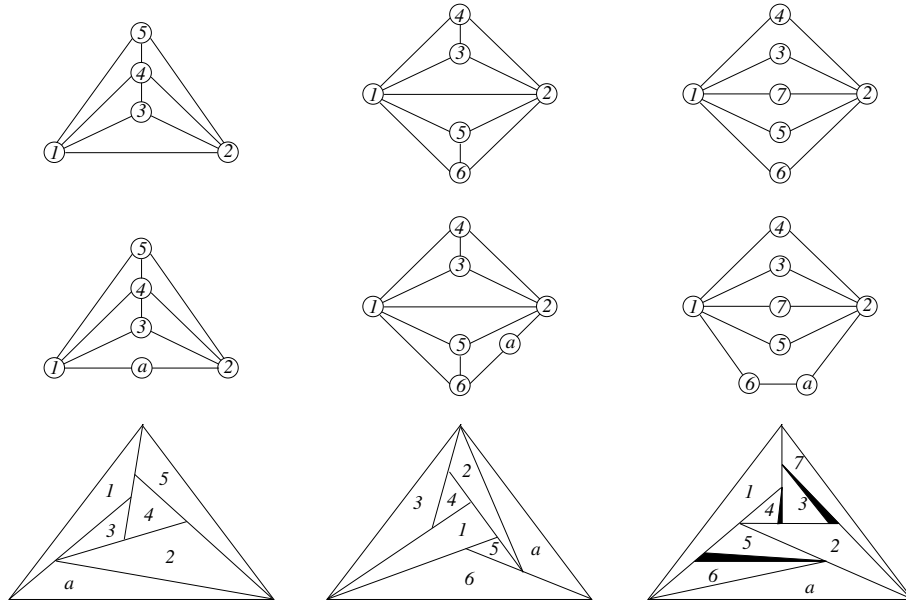


**Fig. 8.** The graphs in the first row (on 5, 6, 7 vertices) do not have touching triangle graph representations. However, subdividing one edge from each, as in the second row, results in graphs that have *TTG* representations. These representations are shown in the third row.

### Omitted Proof

**Theorem 5.** Let  $G$  be a *TTG*, and let  $u$  and  $v$  be any two nodes in  $G$ . Then  $|N_{uv}| \leq 4$  and  $|E_{uv}| \leq 2$ .

**Proof:** Let  $T_u$  and  $T_v$  be the two triangles corresponding to nodes  $u$  and  $v$ . We have already dealt with the two triangles sharing a side above. So, we then consider the case when a pair of sides are collinear, as illustrated in Figure 9.

For this case, we can place a triangle touching  $\vec{12}$  and  $\vec{ab}$ . Since both triangles are to the left of both  $\vec{12}$  and  $\vec{ab}$ , these sides cannot be used in any other feasible angle. There can be no feasible angle formed by  $\vec{23}$  and  $\vec{ca}$ , since, if any part of  $\vec{ca}$  is to the right of  $\vec{23}$ , the latter must be to the left of  $\vec{ca}$ , and vice versa. In addition, there can only be one of the two possible feasible angles formed by  $\vec{23}$  and  $\vec{bc}$  or by  $\vec{31}$  and  $\vec{ca}$ . Thus, there

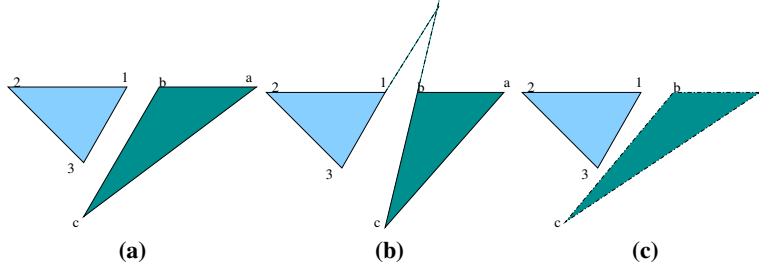


**Fig. 9.** Collinear sides (a)  $\vec{31}$  and  $\vec{bc}$  parallel; (b)  $\vec{31}$  and  $\vec{bc}$  meeting above; (c)  $\vec{31}$  and  $\vec{bc}$  meeting below.

can be at most three touching triangles. (A more careful analysis shows that case (a) can have at most two, while cases (b) and (c) will have three only if the triangles touch.)

For the next case, we consider when a vertex of one triangle touches the interior of a side of the other, as shown in Figure 10. The dotted lines indicate the lines  $\vec{23}$  and  $\vec{31}$ , and divide the area into three regions. We consider the cases determined by which regions contain vertices  $a$  and  $b$ . We note that if  $a$  is in region I,  $b$  must also be in that region. We can also assume that both  $a$  and  $b$  do not lie on either  $\vec{23}$  and  $\vec{31}$ , as this was covered by the collinear case addressed above. In all cases, we have feasible points determined by  $\vec{12}$  with both  $\vec{ca}$  and  $\vec{bc}$ . Also, in all cases either  $\vec{ca}$  is to the left of  $\vec{23}$ , or vice versa, so this pair is eliminated. The similar condition holds for  $\vec{bc}$  and  $\vec{31}$ .

For the case when  $\vec{ab}$  lies in region II (Figure 10(a)),  $\vec{12}$  can also form a feasible point with  $\vec{ab}$ . On the other hand, the triangle  $abc$  lies to the left of both  $\vec{23}$  and  $\vec{31}$ , so we are limited to three feasible points.

When  $\vec{ab}$  lies in region I (Figure 10(b)), the triangle  $abc$  is to the left of  $\vec{31}$ , so the latter has no feasible points. There is always a feasible point fixed by  $\vec{23}$  and  $\vec{bc}$ . If  $\vec{12}$  is to the left of  $\vec{ab}$ , the only remaining possibility is given by  $\vec{ab}$  and  $\vec{23}$ . If  $\vec{12}$  is partly to the right of  $\vec{ab}$ , both  $\vec{ab}$  and  $\vec{23}$  and  $\vec{ab}$  and  $\vec{12}$  give feasible points, but a triangle placed at one blocks the other (and the feasible point of  $\vec{23}$  and  $\vec{bc}$  as well). Thus, we are limited to four touching triangles.

The case when  $\vec{ab}$  lies in region III (Figure 10(c)) is symmetric.

We next consider  $b$  in region I and  $a$  in region II (Figure 10(d)). The triangle  $abc$  is to the left of  $\vec{31}$ , so the latter has no feasible points. In addition,  $\vec{23}$  is to the left of  $\vec{ab}$ , leaving at most four feasible points.

If we leave  $a$  in region II but move  $b$  to region III (Figure 10(e)), we have a similar situation, with triangle  $abc$  is to the left of  $\vec{23}$  and  $\vec{ca}$  is to the left of  $\vec{31}$ .

Switching their roles, with  $a$  in region III and  $b$  in region II (Figure 10(f)), we still have triangle  $abc$  is to the left of  $\vec{23}$  but now  $\vec{31}$  is to the left of  $\vec{ab}$ .

In the final sub-case,  $b$  lies in region I and  $a$  lies in region III (Figure 10(g)). Here, the triangle  $123$  lies to the left of  $\vec{ab}$ , eliminating all feasible points involving the latter. We are left with two remaining possibilities:  $bc$  with  $\vec{23}$  and  $\vec{ca}$  with  $\vec{31}$ , for a total of four.

Next, we assume the triangles touch at two vertices, as shown in Figure 11. There can be a feasible point formed by  $\vec{23}$  and  $\vec{ca}$ , and one by  $\vec{31}$  and  $\vec{bc}$ . On the other hand, we can immediately eliminate the pairs  $\vec{23}$  and  $\vec{bc}$ , and  $\vec{31}$  and  $\vec{ca}$ . If  $\vec{ab}$  is in the left half plane of  $\vec{12}$  (Figure 11(a)), the latter has no feasible points. Thus, there can be at most

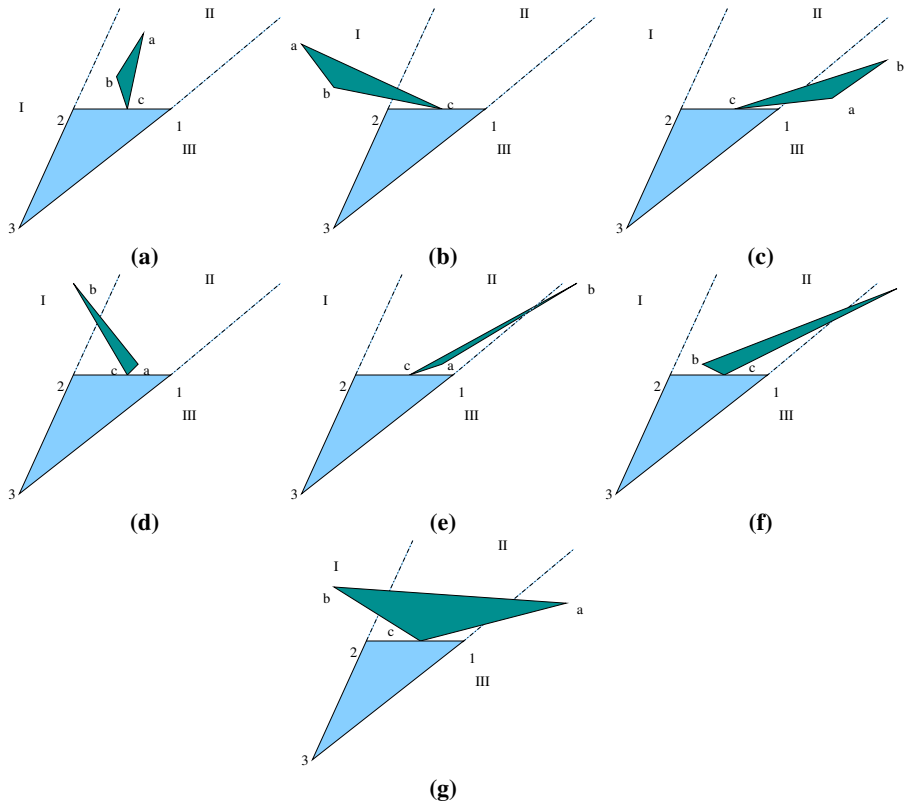


**Fig. 10.** Triangles touch at vertex and side. (a)  $\vec{ab}$  to region II; (b)  $\vec{ab}$  in region I; (c)  $\vec{ab}$  in region III; (d)  $b$  in region I,  $a$  in region II; (e)  $b$  in region III,  $a$  in region II; (f)  $b$  in region II,  $a$  in region III; (g)  $b$  in region I,  $a$  in region III.

four. In fact,  $\vec{ab}$  can have at most one feasible point, with either  $\vec{31}$  or  $\vec{23}$ , but not both, so there are at most 3 feasible points.

Otherwise, either point  $a$  or point  $b$  is to the right of  $\vec{12}$  (Figure 11(b)), all of triangle 123 is to the left of  $\vec{ab}$ , and the symmetric case holds, with no feasible points associated with  $\vec{ab}$ , and at most one additional feasible point formed by  $\vec{12}$  and either  $\vec{ca}$  or  $\vec{bc}$ .

Finally, if the triangles do not touch at all and do not have a pair of collinear sides, consider a pair of closest points  $p_0$  and  $p_1$ , one on each triangle, and the line segment between the two points. If we imagine translating the points along this line segment until the triangles touch, we have one of the three situations: that of Theorem 4, Figure 10 or Figure 11, and similar analysis apply, but with a possible reduction in usable feasible points. For example, consider the configuration of Figure 10(c).

This fits the pattern of Figure 11(a). Thus,  $\vec{12}$  has no feasible points, and  $\vec{ab}$  might potentially form a feasible point with  $\vec{23}$  or  $\vec{31}$ , but not both. Now, unlike the touching case, we have four feasible points from sides  $\vec{23}$ ,  $\vec{31}$ ,  $\vec{bc}$  and  $\vec{ca}$ . The problem is that, if a triangle is placed at one of those points, the remainder become unusable. Thus, we end up with at most three neighboring triangles. To complete the proof, we note that, in all

of the cases, there can be at most two pairs of touching triangles among the ones added.  $\square$

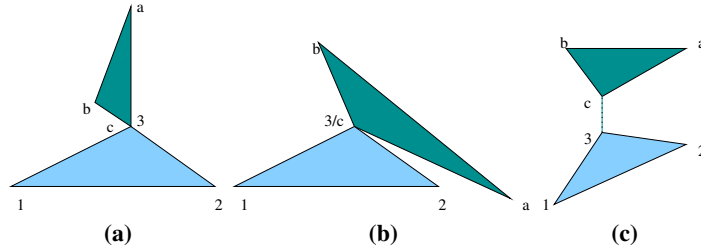


**Fig. 11.** Triangles touch at two vertices (a)  $\vec{ab}$  to the left of  $\vec{12}$ ; (b)  $\vec{ab}$  crossing  $\vec{12}$ ; (c) shows one case of non-touching triangles.

Figures 10 and 11 show that the bounds of 3 or 4 derived in the proof are tight. Theorem 5 shows that the top right graph in Figure 8 is not *TTG*. Although these two theorems provide simple tests for eliminating potential *TTGs*, we are fairly certain that they do not provide sufficient conditions.